ChemComm

Accepted Manuscript

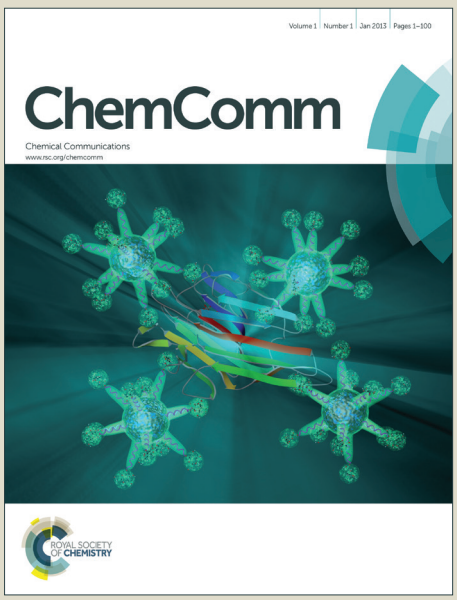

ROYAL SOCIETY OF CHEMISTRY

www.rsc.org/chemcomm

Journal Name

RSCPublishing

COMMUNICATION

Rational design of signal-on biosensors by using Photoinduced Electron Transfer between Ag Nanoclusters and split G-quadruplex halves/Hemin Complex

Cite this: DOI: 10.1039/x0xx00000x

Received 00th January 2012,
Accepted 00th January 2012

DOI: 10.1039/x0xx00000x

www.rsc.org/

Kai Zhang,* Ke Wang, Xue Zhu, Yun Gao, and Minhao Xie*

Photoinduced electron transfer (PET) between DNA/Ag nanoclusters (AgNCs) and G-quadruplex halves/hemin has been used for the building a new sensing platform for the signal-on detection of adenosine and RNA.

Molecular clusters of pure metals, such as gold and silver, are a new class of fluorophores and have great potential for applications in biomedicine.[1-4] Silver nanoclusters own an appealing set of features that complements the properties of organic dyes and quantum dots.[5] They have desirable photophysical properties and low toxicity suitable for biological applications.[6] In recent years, oligonucleotide-templated silver nanoclusters (AgNCs) have attracted special attention due to their facile synthesis, tunable fluorescence emission, and high photostability.[7, 8] They have been used to detect various biologically important analytes based on different signal-transducing mechanisms. However, the scarcity of efficient and accurate approaches for modulating the fluorescence of DNA/AgNCs restricts their potential for general application in biomolecules analysis.[2] On the other hand, the use of G-quadruplex/hemin complexes for biosensor design has become an interesting research topic that enables structure-tailoring and function-expanding of well-developed functional DNA molecules toward more versatile applications.[9-11] Wang and co-works reported a new proof-of-concept that photoinduced electron transfer (PET) between DNA/AgNCs and G-quadruplex/hemin complexes, accompanied by a decrease in the fluorescence of DNA/AgNCs.[2] This strategy has already been used to develop a nanocluster-based molecular beacon (NMB) for the detection of target biomolecules. However, this "signal-off" strategy was proposed based on the quenching mode, which is not preferred in practice because there were a variety of ligands or solvents that may interfere with PET, leading to "false positive" results.

In the present study, we report on the integration of DNA/AgNCs and G-quadruplex halves/hemin complexes and the implementation of these strategy based on PET phenomenon for the development of aptasensors and RNA sensors. We specifically apply the tunable PET properties of this strategy to demonstrate the multiplexed analysis of adenosine. We also apply the nucleic-acid-functionalized Ag/NCs to assay RNA of let-7a. In contrast to related DNA/AgNCs and G-quadruplex/hemin complexes-based aptasensor or nucleic acid sensors that have implemented the PET properities, the present study allows the simple tethering of the specific oligonucleotides stabilizing the AgNCs to the nucleic acid probes. This novel strategy also allows our architecture to be not only "signal-on" but also cost-effective.

The analysis of adenosine by the DNA/AgNC-G-quadruplex halves/ hemin system is depicted schematically in Scheme 1A. The hybridization region of DNA1 (blue) can basepair with hybridization region of DNA3 (yellow) to form a rigid duplex spacer and a DNA-templated loop which is used for the formation of the DNA/Ag NCs within the sensor structure. G-quadruplex halves (black) are two halves of a split DNAzyme that, once recombined, constitutes a signal-quenching element in the sensor module. The recognition part (green) is quite flexible in the absence of the target and allows G-quadruplex halves to freely approach each other and form an intact G-quadruplex at the help of potassium ions (K^+) upon hemin binding which results in the quenching of the fluorescence of the DNA/Ag NCs. Of note, the G-quadruplex halves assembled into G-quadruplex in the presence of Na^+ and K^+ ions in solution, but it forms very fast in K^+ ions solution and slowly in Na^+ ions containing solution.[12] If adenosine is present in the assay solution at the beginning, the recognition part will transform into a special compact secondary structure upon recognizing the target, which, under the help of the duplex spacer, will be able to keep the two part of G-quadruplex halves stay at a distance from each other. Therefore, further addition

of hemin in the presence of potassium ions will not leads to the formation of a recombined G-quadruplex, which leads to the retaining of the fluorescence of the DNA/Ag NCs.

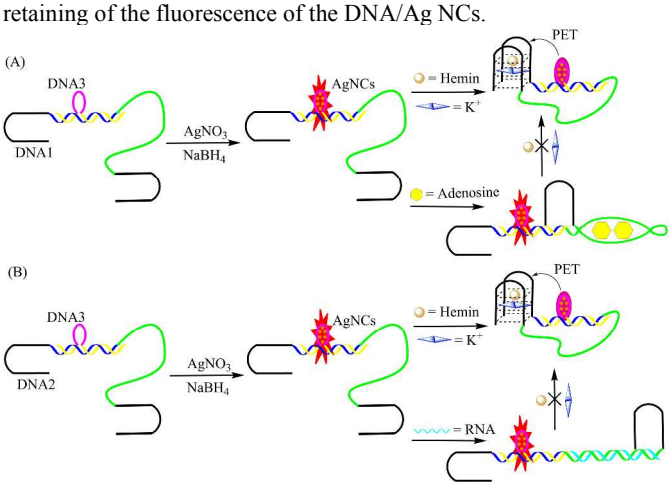

Scheme 1 Schematic Illustrations of the analysis of adenosine (A) and RNA (B) using DNA/AgNC-G-quadruplex halves/hemin complex.

The PET effect was highly sensitive to the position of the DNA/Ag NCs away from the 3 prime end of DNA3. DNA1/DNA3 were performed on a series of probe DNA strands formed by changing the position of the DNA-templated loop from zero to eight bases away from the 3 prime end of DNA3 (Fig. S1). As shown in Fig. S2, the best quenching efficiency was obtained when the DNA-templated loop was four based away from the 3 prime end. This interesting phenomenon may be caused by the stability of DNA1/DNA3 and the distance between AgNCs and G-quadruplex halves/ hemin. The 3 prime end of DNA3-zero and DNA3-two may cannot hybridize with DNA1 effectively, which makes DNA-templated loop "free" in the solution, leading to the AgNCs far away from G-quadruplex halves/ hemin. DAN3, DNA3-six and DNA-eight may hybridize with DNA1 effectively and the quenching efficiency was decreased with the increasing of the distance between G-quadruplex halves/ hemin and AgNCs.

The effects on the synthesis of fluorescent AgNCs, such as pH, was investigated. The pH value, which was controlled by the addition of NaOH or HCl in the experiments, played an important role in the synthesis of the fluorescent AgNCs. As shown in Fig. S3, we obtained the maximum emission intensity when the initial pH of the initial solution is around 4.5. But, to low pH may influence the biological detection of the target; to high pH value causes a negative impact on the intensity, since the high pH may leads to nonofluorescent precipitates of AgOH appeared. So, we chose pH 7.4 as the optimal pH for the following experiments.

In order to achieve optimal assay conditions, the Ag nanoclusters formation time after added $NaBH_4$ was optimized. As displayed in Figure S4A, the fluorescence intensity of the mixture increase rapidly with increasing reaction time in the range from 0 to 14 h and reaches a plateau thereafter. In addition, previous work show that Ag nanoclusters can be oxidized overtime,[13,14] but the fluorescence intensity have no obviously decrease in this work. To ensure complete reduction reactions and preventing oxidation reaction, the reaction time of 14 h was selected for subsequent experiments. Moreover, time-dependent fluorescence intensities decreasing after addition of the K^+ and hemin were measured. The fluorescence intensity of the AgNCs decreases after addition of K^+ and hemin. As shown in Figure S4B, after about 120 min, the quenching reaction of hemin reaches saturation. So a time interval of 120 min was fixed for the quenching reaction.

To verify the feasibility of quantitative detection, the fluorescence changes in the emission of AgNCs under different conditions were investigated. As shown in Fig. 1A, the emission (at 655 nm) of DNA1-DNA3 duplex (curve a) and DNA1-DNA3 duplex/hemin (curve b) was relatively low. The formed DNA1-DNA3 duplex/Ag NCs showed strong fluorescence intensity (curve c). After the introduction of hemin to DNA1-DNA3 duplex/AgNCs (curve d), the fluorescence intensity decreased sharply. This result indicated that the excited electrons of the DNA/AgNCs can be transferred to the hemin complex[2] in our strategy. Upon addition of 80 μM adenosine before the formation of G-quadruplex, the fluorescence intensity increased sharply (curve e). However, upon addition of 80 μM adenosine after the formation of G-quadruplex, the fluorescence it produced signal intensity (curve f) only slightly larger than the background (curve d), which was markedly lower than that of 80 μM of adenosine added ahead. The most likely reason for this is that the formation of the intact G-quadruplex forbids the recognition of adenosine. This result indicates that the target adenosine could combine with the recognition part, forbidding the G-quadruplex halves/hemin complex to form, which resulted in an increase in the fluorescence intensity. Fig. 1B shows the fluorescence emission spectra of DNA/AgNC-G-quadruplex halves/hemin complex in the presence of different concentrations of target adenosine. As the concentration of adenosine increased, the fluorescence intensity obviously increased. Fig. 1C shows the relationship between the fluorescence intensity and the concentration of adenosine. A good linear range from 0 to 80 μM with an equation Y= 10.65 X+78.65 (R^2=0.994), where Y is the fluorescence intensity and X is the concentration of adenosine, and a detection limit of 1.0 μM could be obtained according to the responses of the blank tests plus 3 times the standard deviation (3σ) (Fig. 1C inset); its sensitivity is much better than or comparable to those of fluorescent dye-based sensing approaches.[15, 16] To test the specificity of this sensing system, other adenosine analogues guanosine, uridine, and cytidine were also investigated (Fig. 1D). It was found that adenosine resulted in an obvious change in the fluorescence, while the fluorescence changes in the presence of the analogues were nearly negligible. These results demonstrate that this approach exhibits excellent selectivity for adenosine detection over competing nucleosides.

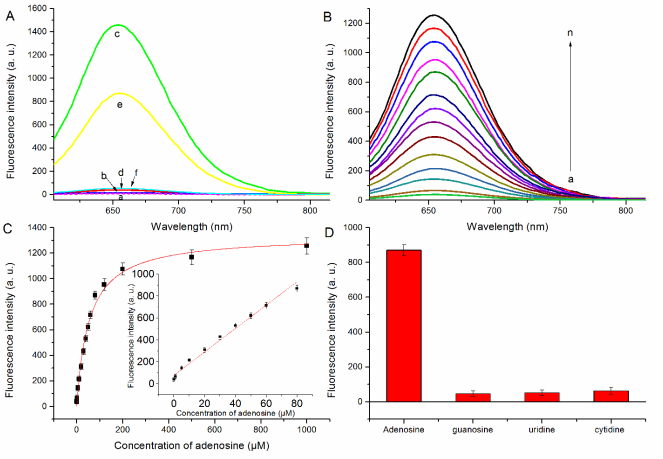

Fig. 1 (A) Emission spectra of DNA/AgNCs under different conditions: (a) DNA1-DNA3 duplex; (b) DNA1-DNA3 duplex/hemin; (c) DNA1-DNA3 duplex/AgNCs; (d) DNA1-DNA3 duplex/hemin/AgNCs; (e) DNA1-DNA3 duplex/hemin/AgNCs treated with 80 μM adenosine; and (f) DNA1-DNA3 duplex/hemin/AgNCs treated with 80 μM adenosine after the adding of hemin. (B) Fluorescence emission spectra at different adenosine concentrations (0, 1, 5, 10, 20, 30, 40, 50, 60, 80, 120, 200, 500, and 1000 μM from a to n). (C) Relationship between the fluorescence

intensity and the concentration of adenosine. The inset shows the linear relationship over the concentration range from 0 to 80 μM. (D) Selectivity of target adenosine analysis.

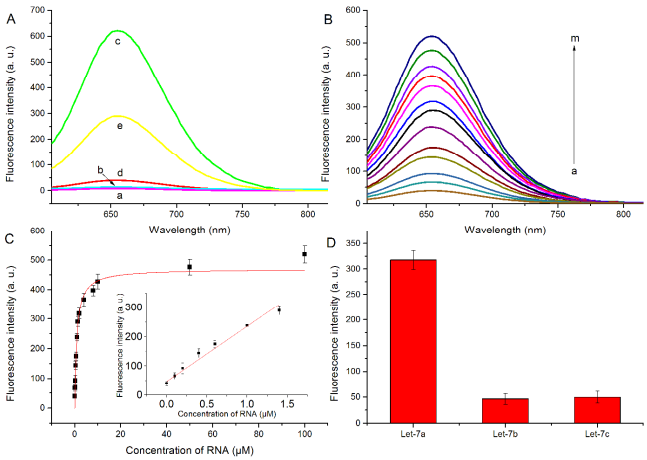

Fig. 2 (A) Emission spectra of DNA/AgNCs under different conditions: (a) DNA2-DNA3 duplex; (b) DNA2-DNA3 duplex/hemin; (c) DNA2-DNA3 duplex/AgNCs; (d) DNA2-DNA3 duplex/hemin/AgNCs; and (e) DNA2-DNA3 duplex/hemin/AgNCs treated with 1.4 μM let-7a. (B) Fluorescence emission spectra at different RNA concentrations (0, 0.1, 0.2, 0.4, 0.6, 1.0, 1.4, 2.0, 4.0, 8.0, 10, 50 and 100 μM from a to m). (C) Relationship between the fluorescence intensity and the concentration of let-7a. The inset shows the linear relationship over the concentration range from 0 to 1.4 μM. (D) Selectivity of target RNA analysis.

To demonstrate further the feasibility and universality of present proof-of-concept, a homogeneous model was adopted for detection of RNA with just a little change in the sensing sequence. As shown in Scheme 1B, the G-quadruplex halves sequences (black) assembles into a probe consisting of the hybridization region (blue) and a single-stranded oligonucleotide recognition part complementary to the target RNA, let-7a (green) (Fig. S1). Formation of the hybridization of the target RNA with the recognition part keep the two part of G-quadruplex halves stay at a distance from each other. Therefore, further addition of hemin in the presence of potassium ions will not lead to the formation of a recombined G-quadruplex, which leads to the retaining of the fluorescence of the DNA/Ag NCs.

The feasibility of the experimental principle was examined under different conditions. From the results shown in Fig. 2A, we could conclude that the let-7a indeed hybridized with the recognition part of DNA2 and forbade the formation of the G-quadruplex/hemin complex, resulting in the unchanged in the fluorescence intensity. We further explored the fluorescence emission spectra of the DNA/Ag NC−G-quadruplex/hemin interaction in the presence of different concentrations of RNA (Fig. 2B). The results showed that as the RNA concentration increased, the fluorescence intensity increased accordingly. Fig. 2C shows the relationship between the fluorescence intensity and the RNA concentration, and the inset shows the calibration curve for quantitative analysis of RNA. The intensity was linearly dependent on the concentration of RNA over the range from 0 to 1.4 μM with an equation Y= 187.76 X+47.65 (R^2= 0.979), where Y is the fluorescence intensity and X is the concentration of RNA, and a detection limit of 0.1 μM could be obtained according to the responses of the blank tests plus 3 times the standard deviation (3σ); this was lower than or comparable to the detection limits for most of the previously reported AgNCs based sensor for RNA detection.[17] Similarly, to test the specificity of this sensing system, three members of let-7 family (let-7a, let-7b, and let-7c), which only one- or two-nucleotide differences out of 22 nucleotides between them, are selected as the detection model. Fig. 2D shows the fluorescence changes for the target RNA and the mismatched DNA strands. These results clearly demonstrate that the detection approach shows a high selectivity toward the target RNA. Moreover, we observed that miRNA (let-7c) with the single-base mismatch at the 3 prime end caused slightly increased fluorescence intensity. Such intensity of fluorescence intensity (49.6) was much smaller than that for the perfectly matched miRNA (317.7) with a discrimination ratio > 6. This high specificity with mismatch discrimination ability was derived from the recognition part-miRNA hybridization step, which was dominated by the perfect match at the 3 prime end and highly dependent upon the hybridization stability between the target and the recognition part.

Conclusions

In conclusion, we have demonstrated a new signal-on strategy involving PET between DNA/Ag NCs and G-quadruplex halves/hemin complexes that can be used as a sensor for the sensitive and selective detection of adenosine and RNA. Compared with conventional methods, this proposal shows some unique features: (1) It is very simple and does not require separation and troublesome procedures. (2) It does not involve any chemical modification of DNA, as DNA-templated silver nanoclusters serve as signal indicators and the G-quadruplex/hemin complex as the acceptor, which makes it simple and low-cost. (3) It can be used for multiple targets with only small changes in the sequence of recognition part. More important, this strategy validates a successful paradigm for exploring new and interesting properties of functional nanomaterials and thus extending their applications in multiple fields.

This work is supported by the Social Development Fund of Jiangsu Province (BE2013614), the Grants from National Natural Science Foundation (81300787), the Natural Science Foundation of Jiangsu Province (BK2011168, BK2012105, BK20041103), the Technology Infrastructure Plan of Jiangsu Province-Technology Public Service Platform (BM2012066) and the Youth Foundation of Jiangsu Institute of Nuclear Medicine.

Notes and references

Key Laboratory of Nuclear Medicine, Ministry of Health, Jiangsu Key Laboratory of Molecular Nuclear Medicine, Jiangsu Institute of Nuclear Medicine. Wuxi, Jiangsu 214063, China. Fax: +86-510-85508775; Tel: +86-510-85508775; E-mail: zhangkai@jsinm.org (K. Zhang), xieminhao@jsinm.org (M. Xie)

Electronic Supplementary Information (ESI) available: Experimental details, oligonucleotide sequences and quenching efficiency of the position of the DNA-templated loop. See DOI: 10.1039/c000000x/

1. J. Liu, *TrAC, Trends Anal. Chem.*, 2014, **58**, 99-111.
2. L. Zhang, J. Zhu, S. Guo, T. Li, J. Li and E. Wang, *J. Am. Chem. Soc.*, 2013, **135**, 2403-2406.
3. K. Zhang, K. Wang, X. Zhu, J. Zhang, L. Xu, B. Huang and M. Xie, *Chem. Commun.*, 2014, **50**, 180-182.
4. W.-Y. Chen, G.-Y. Lan and H.-T. Chang, *Anal. Chem.*, 2011, **83**, 9450-9455.
5. X. Liu, F. Wang, R. Aizen, O. Yehezkeli and I. Willner, *J. Am. Chem. Soc.*, 2013, **135**, 11832-11839.
6. M. Zhang, S.-M. Guo, Y.-R. Li, P. Zuo and B.-C. Ye, *Chem. Commun.*, 2012, **48**, 5488-5490.
7. W. Guo, J. Yuan and E. Wang, *Chem. Commun.*, 2011, **47**, 10930-10932.
8. W. Guo, J. Yuan, Q. Dong and E. Wang, *J. Am. Chem. Soc.*, 2009, **132**, 932-934.
9. W. Zhou, X. Gong, Y. Xiang, R. Yuan and Y. Chai, *Anal. Chem.*, 2013, **86**, 953-958.

10. Y. Huang, J. Chen, S. Zhao, M. Shi, Z.-F. Chen and H. Liang, *Anal. Chem.*, 2013, **85**, 4423-4430.
11. K. Zhang, X. Zhu, J. Wang, L. Xu and G. Li, *Anal. Chem.*, 2010, **82**, 3207-3211.
12. A. D. Rodrigues Pontinha, A.-M. Chiorcea-Paquim, R. Eritja and A. M. Oliveira-Brett, *Anal. Chem.*, 2014, **86**, 5851.
13. K. Morishita, J. L. MacLean, B. Liu, H. Jiang and J. Liu, *Nanoscale*, 2013, **5**, 2840.
14. S. Walczak, K. Morishita, M. Ahmed and J. Liu, *Nanotechnology*, 2014, **25**, 155501.
15. L.-L. Li, P. Ge, P. R. Selvin and Y. Lu, *Anal. Chem.*, 2012, **84**, 7852-7856.
16. Y. Xiang, A. Tong and Y. Lu, *J. Am. Chem. Soc.*, 2009, **131**, 15352-15357.
15. S. W. Yang and T. Vosch, *Anal. Chem.*, 2011, **83**, 6935-6939.